Cosmological magnetic fields from primordial helical seeds

Günter Sigl
GReCO, Institut d'Astrophysique de Paris, CNRS, 98bis Boulevard Arago, 75014 Paris, France
(Received 22 February 2002; revised manuscript received 26 August 2002; published 18 December 2002)

Most early universe scenarios predict negligible magnetic fields on cosmological scales if they are unprocessed during subsequent expansion of the universe. We present a new numerical treatment of the evolution of primordial fields and apply it to weakly helical seeds as they occur in certain early universe scenarios. If seed fields created during the electroweak phase transition have close to thermal strength and coherence lengths a few orders of magnitude below the horizon scale, initial helicities not much larger than the baryon to photon number can lead to fields of $\sim 10^{-13}$ G at scales up to 100 parsec today.

DOI: 10.1103/PhysRevD.66.123002 PACS number(s): 98.62.En, 95.30.Qd, 98.80.Cq

I. INTRODUCTION

The origin of galactic and large scale extragalactic magnetic fields (for which there is no detection yet on scales larger than megaparsec) is one of the main unresolved problems of astrophysics and cosmology [1]. In most scenarios where magnetic fields are produced in the early universe, these seed fields are concentrated on scales below the horizon scale where they dissipate quickly and are too small on cosmological scales to have any observable effects. However, if pseudo-scalar interactions induce a nonvanishing helicity of these seeds, such as in string cosmology [2] or during the electroweak phase transition by projection of a non-Abelian Chern-Simons number onto the electromagnetic gauge group [3–5], then part of the small scale power can cascade to large scales and produce observable effects [6,4,7,8]. The full magnetohydrodynamics description of such nonlinear cascades can usually be treated numerically only in a very limited range of length and time scales [9]. However, under certain conditions the problem can be formulated in terms of Gaussian correlation functions. In the present paper we apply this approach which allows us to numerically follow magnetic field evolution over the large range of length and time scales involved between production of helical seed fields in the primordial universe and today. We use natural units throughout, $\hbar = c = k = 1$. All quantities are thus expressed in powers of GeV and can be expressed in more familiar units be applying suitable conversion factors.

II. MAGNETOHYDRODYNAMICS IN THE EARLY UNIVERSE

The principal equations for magnetic field **B** and velocity field **v** in the one-fluid approximation of magnetohydrodynamics (MHD) are [10]

$$\partial_t \mathbf{B} = \boldsymbol{\nabla} \times (\mathbf{v} \times \mathbf{B} - \eta \boldsymbol{\nabla} \times \mathbf{B}),$$

$$\partial_t \mathbf{v} + (\mathbf{v} \cdot \boldsymbol{\nabla}) \mathbf{v} = \frac{(\boldsymbol{\nabla} \times \mathbf{B}) \times \mathbf{B}}{4\pi\rho}, \tag{1}$$

where η is the resistivity and ρ is the fluid density. The second equation describes the Lorentz force $\mathbf{f} = [(\boldsymbol{\nabla} \times \mathbf{B}) \times \mathbf{B}]/(4\pi)$ of the magnetic field on the flow. To eliminate it, following Refs. [4,11], we split the velocity field into an external flow $\mathbf{v}_e$ and a back-reaction term:

$$\mathbf{v} \sim \mathbf{v}_e + \tau \frac{\mathbf{f}}{\rho} = \mathbf{v}_e + \frac{\tau}{4\pi\rho} (\boldsymbol{\nabla} \times \mathbf{B}) \times \mathbf{B}. \tag{2}$$

Here, τ is the fluid response time to the Lorentz force and can be viewed as the time the charged fluid can be accelerated until it interacts (scatters) with other particles in the background and therefore describes damping of the magnetic field modes. The external flow $\mathbf{v}_e$ is then uncorrelated with the magnetic field in this approximation. Note that the Lorentz force term implies that $\langle \mathbf{v} \times \mathbf{B} \rangle$ does not vanish, as required for a nontrivial effect of the first term in the equation for $\partial_t \mathbf{B}$.

Again following Ref. [11], we express the magnetic field in terms of two-point correlation functions $M_{ij}(r,t) = \langle B_i(\mathbf{x},t) B_j(\mathbf{y},t) \rangle$, where $r = |\mathbf{x} - \mathbf{y}|$, assuming isotropy and homogeneity:

$$M_{ij} = M_N \left(\delta_{ij} - \frac{r_i r_j}{r^2} \right) + M_L \frac{r_i r_j}{r^2} + H \epsilon_{ijk} r_k, \tag{3}$$

where M_L, M_N, and H are longitudinal, transverse, and helical magnetic correlation functions, respectively. $M_N = \partial_r (r^2 M_L)/(2r)$ is not independent because of $\boldsymbol{\nabla} \cdot \mathbf{B} = 0$. We define the magnetic field and gauge invariant helicity power spectra per logarithmic wave-number interval $b^2(k)$ and $h(k)$ by $E_M \equiv \langle \mathbf{B}^2(\mathbf{r}) \rangle/(8\pi) = \int_0^{+\infty} dk b^2(k)/(8\pi k)$ and $H_M \equiv \langle \mathbf{B}(\mathbf{r}) \cdot \mathbf{A}(\mathbf{r}) \rangle = \int_0^{+\infty} dk h(k)/k$, with **A** the vector potential, $\mathbf{B} = \boldsymbol{\nabla} \times \mathbf{A}$. One can show that M_L and H are related to these power spectra via

$$M_L(r) = \int_0^{+\infty} \frac{dk}{k} \frac{j_1(kr)}{kr} b^2(k) \sim b^2(1/r),$$

$$H(r) = -\frac{1}{3r} \int_0^{+\infty} dk\, j_1(kr) h(k) \sim \frac{h(1/r)}{r^2}, \tag{4}$$

where $j_1(x) = \sin(x)/x^2 - \cos(x)/x$ is the first order spherical Bessel function. In terms of the usual Fourier transforms $\mathbf{B}(\mathbf{k}) = \int d^3\mathbf{r}/(2\pi)^{3/2} \exp(i\mathbf{k} \cdot \mathbf{r}) \mathbf{B}(\mathbf{r})$, etc., $b^2(k) = 4\pi k^3 \mathbf{B}^2(k)$ and $h(k) = k^3 \int d\Omega_{\mathbf{k}} \mathbf{B}(\mathbf{k}) \cdot \mathbf{A}(\mathbf{k})$. Equation (4)

also shows that $M_L(0)=8\pi E_M/3$, and $H_M=-3\int_0^{+\infty}drrH(r)$, and $|h(k)|\leq b^2(k)/k$ implies, for all r,

$$|H(r)|\lesssim|M_L(r)|/r\equiv H_{\max}(r). \tag{5}$$

Completely analogous expressions apply for the external flow component which we assume to be incompressible, $\boldsymbol{\nabla}\cdot\mathbf{v}=0$, by substituting $B_i(\mathbf{x},t)\to\mathbf{v}_{ei}(\mathbf{x},t)$, $M_{ij}\to T_{ij}$, $M_N\to T_N$, $M_L\to T_L=\int dt\langle\mathbf{r}\cdot\mathbf{v}_e(0,0)\mathbf{r}\cdot\mathbf{v}_e(\mathbf{r},t)\rangle/r^2$, and $H\to C=\int dt\langle\mathbf{r}\cdot\mathbf{v}_e(0,0)\times\mathbf{v}_e(\mathbf{r},t)\rangle/(2r^2)$. Both the time scales appearing in these integrals and the damping scale τ are assumed small compared to the scale on which M_{ij} changes. In the cosmological context this is the Hubble scale r_H, which in the radiation dominated area at cosmological temperatures $T\gtrsim$ eV is given by $r_H(T)^{-1}\sim m_{\rm P}/T^2\sim 5\times10^{-7}(T/\mathrm{GeV})^{-2}$ s$\sim 1.5\times10^4\,(T/\mathrm{GeV})^{-2}$ cm, where $m_{\rm P}\sim10^{19}$ GeV is the Planck mass [12].

To take into account cosmological expansion we redefine M_L and H as dimensionless variables from now on, $M_L\to M_L/T^4$ and $H\to H/T^5$. Assuming Gaussian correlation functions, arbitrary field products can be expressed in terms of products of two-point correlation functions, and Eqs. (1) and (2) lead to a closed system of partial differential equations for $M_L(r,t)$ and $H(r,t)$ [11],

$$\partial_t M_L=\frac{2}{r^4}[\partial_r(r^4\kappa\partial_r M_L)-M_L\partial_r(r^4\partial_r T_L)]-4\alpha TH,$$

$$\partial_t H=\frac{1}{r^4}\partial_r[r^4\partial_r(2\kappa H+\alpha M_L/T)]. \tag{6}$$

Here,

$$\kappa=\eta+\frac{\tau_{\rm ext}\langle v_e^2\rangle(T)}{3}\left(1-\frac{T_L(r)}{T_L(0)}\right)+\frac{\tau T^4}{2\pi\rho}M_L(0,t),$$

$$\alpha=2C(0)-2C(r)-\frac{\tau T^5}{\pi\rho}H(0,t), \tag{7}$$

where $\tau_{\rm ext}$ is the correlation time scale of the external fluid flow, and all quantities appearing here are in physical (not comoving) coordinates.

The effective diffusion term κ has contributions from microscopic diffusion (η), scale-dependent diffusion from the external flow $\propto\langle v_e^2\rangle$, and from nonlinear drift due to the Lorentz force [term $\propto M_L(0)$]. Note that the latter can be written in a form analogous to the external flow contribution as $(2/3)\tau v_A^2$, where the Alfvén speed v_A is defined by $\rho v_A^2/2\equiv E_M=3T^4M_L(0)/(8\pi)$. The back-reaction term can thus be interpreted as being due to the creation of a bath of Alfvén waves of typical speed v_A which are damped on time scale τ. The α effect includes a scale dependent term $[2C(0)-2C(r)]$ from the external fluid flow and a nonlinear drift term $\propto H(0)$.

Equation (6) describes small and large scale dynamos of helical magnetic fields including damping by ohmic dissipation and "Silk" damping (which is expressed by the redshift dependent relaxation time τ) on a unified basis. In the early universe before photon decoupling, i.e. for $T\gtrsim0.25$ eV, the resistivity can be estimated by $\eta\simeq(n_e/n_\gamma)^{-1}/(40\pi T)$ [13]. Here, the electron to photon ratio n_e/n_γ drops from ~1 to $\sim10^{-9}$ at e^+e^- annihilation, $T\sim20$ keV. Equations (6) and (7) show that resistivities of the order T^{-1}, typical for the early universe, lead to damping within a Hubble time on physical length scales up to the geometric mean of the thermal and Hubble scales,

$$r_\eta\lesssim(\eta T)^{1/2}(T/H)^{1/2}T^{-1}=(\eta T)^{1/2}(H/T)^{1/2}H^{-1}$$

$$\text{where }\ (H/T)^{1/2}\simeq1.6\times10^{-9}\left(\frac{T}{\mathrm{GeV}}\right)^{1/2}. \tag{8}$$

The scale r_η can thus be interpreted as resistive scale in the early universe context. These are scales typical for the creation of seed fields, and thus resistivity has to be taken into account at least at high temperatures. After recombination, i.e., for $T\lesssim0.25$ eV, the Spitzer resistivity $\eta\simeq\pi m_e^{1/2}e^2/T_e^{3/2}$ applies, where m_e, e, and $T_e\sim10^6$ K are electron mass, charge, and temperature, assuming full ionization [10].

If the spatial derivatives of M_L and H fall off faster than $1/r$ for $r\to\infty$, Eqs. (6) and (7) imply $\partial_t H_M=18\eta H(0)$, and thus helicity is conserved in the absence of resistivity. From the above equations one can show that approximate conservation of helicity leads again to the condition that significant magnetic field power and helicity should be concentrated above the resistive scale Eq. (8). We note, however, that this is not an exact condition for helicity conservation due to the other nonlinear terms in Eqs. (6) and (7).

Below e^+e^- annihilation, for $T\lesssim20$ keV, within the MHD one fluid approximation the fluid coupled to the magnetic field is well represented by the tightly coupled remaining free electrons and protons and τ is governed by Thomson scattering of photons off electrons. In this regime we use [14]

$$\tau=\tau_\gamma\simeq4\times10^{21}\left(\frac{0.25\ \mathrm{eV}}{T}\right)^4X_e^{-1}\ \mathrm{cm},$$

$$\frac{\rho}{T^4}\simeq0.4\frac{4\pi^2}{45}\left(\frac{0.25\ \mathrm{eV}}{T}\right)\left(\frac{\Omega_b h^2}{0.0125}\right), \tag{9}$$

where the number of free electrons per nucleon X_e is $\simeq1$ for $T\gtrsim0.25$ eV and $\simeq10^{-5}$ for $T\lesssim0.25$ eV, and $\Omega_b h^2$ is the baryon density in terms of the critical density times the squared Hubble constant in units of 100 km s^{-1} Mpc^{-1} today. For $T\gtrsim20$ keV we can approximate the fluid to consist of the electromagnetically interacting particles and τ is governed by neutrino scattering with [14]

$$\tau=\tau_\nu\simeq10^{11}\left(\frac{\mathrm{MeV}}{T}\right)^5\frac{8.75}{g_r-2}\frac{g_r}{g_\nu}\ \mathrm{cm}, \tag{10}$$

and $\rho/T^4\simeq g_f\pi^2/30$, where g_r, g_f, and $g_\nu=5.25$ are the statistical weights of all relativistic particles, the particles in the fluid, and of the neutrinos, respectively. Note that this is an underestimate once the neutrinos become strongly

coupled to the plasma, $\tau_\nu \ll r_H^{-1}$. We have verified that this does not influence the final results significantly. Finally, whenever τ exceeds the Hubble radius, the latter is used instead.

III. NUMERICAL SIMULATIONS

For any early universe scenario the initial conditions for M_L and H at the temperature where the fields are created should be calculated from the power spectra $b^2(k)$ and $h(k)$, using Eq. (4). The magnetic field evolution can then be obtained by numerically integrating the nonlinear partial differential Eq. (6) in comoving coordinates from this initial time up to redshift zero. This is done by employing an alternating implicit method [15] to a one-dimensional grid of typically 100 bins roughly logarithmic in comoving distance between the inverse cosmic microwave background (CMB) temperature T_0 (which is comovingly constant) and ~ 1 Mpc. We use the logarithm of the temperature $\ln T$ as an independent variable and adopt the standard relations between time and temperature, see, e.g., Ref. [12].

At a physical length scale r at cosmic time t the accuracy (Courant) criterion on the step size is [15] $\Delta \ln T \lesssim r^2/[t \max(\kappa,\alpha)]$. For about 10^4 time steps per decade in T and for the coefficients given by Eq. (7) this is typically fulfilled for comoving lengths down to the parsec scale which are mostly of interest here, and for temperatures up to the electroweak scale. Although this accuracy requirement is not fulfilled at the smallest length scales close to the inverse temperature used in the numerical integration, the implicit method assures at least convergence toward the equilibrium solution at such scales. All simulations presented here start at the electroweak scale, $T = 100$ GeV.

In the following we parametrize the magnetic seed field by

$$M_L(r) = N \frac{8\pi^3}{90} \frac{1}{(1 + r/r_B)^n}, \tag{11}$$

where N characterizes the strength relative to thermal energy density, r_B is the scale on which it is concentrated, and n is the power law index at much larger scales (causally produced fields correspond to $n \geqslant 5$).

IV. HELICAL FIELDS IN THE ABSENCE OF EXTERNAL FLOWS

To demonstrate the general effect of helicity we start with magnetic fields of nonvanishing helicity in the absence of source terms, $\mathbf{v}_e = 0$. We start at the electroweak scale, $T = 100$ GeV, with a seed field Eq. (11) with $N = 0.1$, concentrated at a scale $r_B = 10^{-4} r_H (100 \text{ GeV})^{-1}$ where bubbles of true vacuum are expected to form during the electroweak transition. Seed fields of nearly thermal strength, $N \sim 1$, are not unusual in the early universe, but are usually restricted to thermal length scale $r_B \sim T^{-1}$. However, dynamo effects acting during the electroweak phase transition can push the thermal fields up to the bubble scales [16] which is only a few orders of magnitude below the Hubble scale r_H^{-1}. The

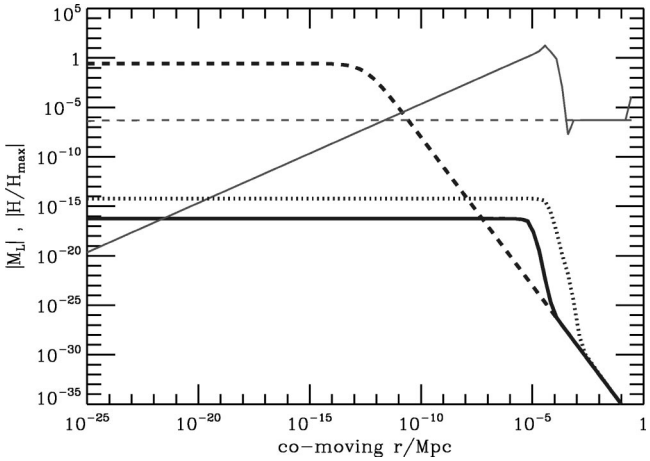

FIG. 1. Results in comoving length scale r for the case without external fluid flow. Thick lines show $M_L(r)$ in units of T^4, for initial condition at $T = 100$ GeV (thick dashed), and at zero redshift (thick solid, i.e., $M_L = 1$ corresponds to a field strength of $\simeq 1.4 \times 10^{-6}$ G today, note that M_L is quadratic in **B**). Thin lines show helicity relative to maximal, $h(r) \equiv H(r)/H_{\max}(r)$, for initial condition (thin dashed), and at zero redshift (thin solid). For comparison, the thin dotted line shows the final $M_L(r)$ for maximal initial helicity (not shown).

contributions of different bubbles are expected to yield a superposition of magnetic dipoles, leading to a power law index $n = 3$ [16]. We assume an initial helicity $H_M \sim 100 n_b$, somewhat larger than the baryon number n_b, as suggested by particle physics arguments [4,5]. Assuming the relative helicity, $h(r) \equiv H(r)/H_{\max}(r)$, to be roughly independent of r, this corresponds to $H(r) \sim 100/N(n_b/n_\gamma)\, M_L(r)/r \simeq 5 \times 10^{-7} H_{\max}(r)$, where the baryon to photon ratio $n_b/n_\gamma \sim 5 \times 10^{-10}$. Figure 1 shows results for M_L and the relative helicity at zero redshift. The magnetic field is decreased by dissipation up to the $\simeq 0.1$ parsec scale, whereas inverse cascades have enhanced the field on scales of a few parsec, reaching $\sim 10^{-14}$ G. The coherence scale is roughly where $M_L(r)$ cuts off and is consistent with analytical estimates [7,8], but significantly larger than in Ref. [5]. For comparison, Fig. 1 also shows the larger enhancement of M_L for maximal initial helicity (the case discussed in Ref. [8]) which, however, we consider speculative in the absence of a specific model predicting such large helicities.

It is easy to show that the total helicity H_M which is dominated by the peak of $h(r)$ in Fig. 1 is indeed roughly conserved, as is suggested by the fact that the magnetic seed field power extends to scales r_B much larger than the resistive scale Eq. (8) in this scenario. Evolution is thus dominated by magnetic back reaction onto the fluid. Indeed, conservation of H_M is usually employed to estimate the field strength via $B^2 \sim H_M/l_c$ which requires an analytical estimate of the coherence scale l_c [5]. In our numerical approach l_c comes out without further assumptions as the scale where the correlation function cuts off. Note that l_c can only grow when B^2 decreases due to dissipation.

Helicity is not expected to be conserved if most of the magnetic field power is concentrated on length scales below

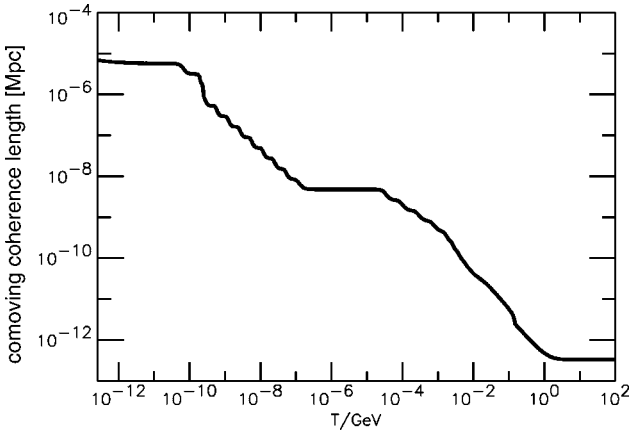

FIG. 2. Evolution of the magnetic field comoving coherence scale $l_c \simeq \int_0^\infty dr r M_L(r) / \int_0^\infty dr M_L(r)$, with temperature. This is for the scenario with a fully helical external fluid flow of small amplitude, $\langle v_e^2 \rangle = 10^{-12}$, before neutrino decoupling.

Eq. (8) where resistivity becomes important. If the seed field power spectrum does not extend beyond these scales, the numerically obtained zero-redshift magnetic field strength is indeed much smaller than in Fig. 1. Furthermore, seed field strengths much weaker than thermal turn out not to lead to significant inverse cascades.

V. NONHELICAL FIELDS WITH HELICAL EXTERNAL FLOW

We now consider helical fluid motion, as it can arise during cosmological phase transitions (see, for example, Refs. [3,4] for the electroweak phase transition). We consider the possible production of baryon and lepton numbers close to unity, $n_b/n_\gamma \sim 1$ at $T \gg 100$ GeV, for instance, during a phase transition related to grand unification, which would also imply almost maximally helical flows [4,5]. These flows would consist of the tightly coupled relativistic electroweak plasma and could survive as a small perturbation at least down to the neutrino decoupling temperature, i.e., $\tau_{\rm ext} \simeq r_H^{-1}$ for $T \gtrsim 1$ MeV. Their amplitude can be estimated by the dilution factor $\langle v_e^2 \rangle \sim (n_b/n_\gamma)^{4/3}_{\rm today} \sim 10^{-12}$ due to the necessary entropy production above the electroweak scale. We thus assume $T_L(0) = r_H^{-1} \langle v_e^2 \rangle / 3 \sim 10^{-12} r_H^{-1}$ for $T > 1$ MeV, and zero below. It turns out that the final results are quite insensitive to the behavior of $T_L(r)$ for $r > 0$, as long as it falls off rapidly, as expected for a relic flow from mechanisms acting far above the electroweak scale where the horizon is microscopic. We again start the simulation at the electroweak transition, and with the same magnetic field as above, but this time with vanishing initial helicity, $H(r) \equiv 0$. The magnetic field develops helicity and its final spectrum today is very similar to the fully helical case of Fig. 1, reaching values close to 10^{-13} G up to about 10 parsec. Figure 2 shows the growth of the coherence scale as a function of T for this case (an analogous figure for the cases of Fig. 1 would be very similar). Since $T \propto t^{-1/2}$ during radiation domination, the coherence scale scales as t^p with $p = 1/2$–$2/3$ in this regime, except for $100\,{\rm eV} \lesssim T \lesssim 100$ keV, i.e., for a certain period after e^+e^- annihilation where resistivity increases rapidly by a factor $\sim 10^9$. These indices are also consistent with analytical estimates [7,8]. In the matter dominated regime, $T \lesssim 1$ eV, the coherence scale does not increase significantly anymore.

Our results also demonstrate that the presence of helicity above the resistive scale Eq. (8) prevents complete dissipation of the fields below the resistive scale, resulting in a flat correlation function up to the coherence scale. Furthermore, the relative magnetic helicity rises linearly with r and is close to maximal at the coherence scale. This could have ramifications for the actual detection of helicity, for example, via its effects on the CMB [17] and could be an important signature of physics at or above the electroweak scale.

VI. CONCLUSIONS

We used the evolution equations for the two-point correlation function of helical magnetic fields in MHD approximation including magnetic diffusion, fluid viscosity, and back reaction onto the external fluid to evolve weakly helical fields produced in the early universe up to today. We find that magnetic fields and/or fluid flows with a relative helicity not much larger than the baryon to photon number $\sim 10^{-9}$, as expected during the electroweak period, can lead to significant inverse cascades. This is true as long as the seed fields are close to thermal in strength and have significant power on length scales above the resistive scale Eq. (8) $r_\eta \simeq 2 \times 10^{-9} (T/100\ {\rm GeV})^{1/2} r_H^{-1} \simeq 8 \times 10^6 (T/100\ {\rm GeV})^{-1/2} T^{-1}$, where resistivity is negligible and helicity is conserved. Under these conditions which are met in scenarios such as in Ref. [16], magnetic fields can be enhanced by several orders of magnitude compared to the merely redshifted and frozen-in initial fields at scales in the parsec and kiloparsec range today. If the seeds are roughly thermal in strength and if their power is concentrated on scales not much smaller than the horizon scale around the electroweak transition, the coherence length can be 10–100 parsec with field strengths up to 10^{-13} G. While this is smaller than the analytical estimates in Ref. [8], it is based on the more realistic assumptions of small helicities of order the baryon to photon number where fluid viscosity cannot be neglected. The fields we obtain are certainly larger than from ''astrophysical'' seed field mechanisms such as the Biermann battery, but are also well within the limits from big bang nucleosynthesis and the CMB (the best of which are $\sim 10^{-9}$ G on kpc–Mpc scales, see, e.g., [18–20]), and from gravity wave production [$B(r) \lesssim 10^{-11} (r/100\ {\rm pc})^{-3}$ G for $n = 3$ [21]]. The fields we obtain may be dominant in voids and outside of galaxy concentrations where pollution from astrophysically produced fields are negligible. In such areas they may, for example, have important effects on ultrahigh energy cosmic ray propagation [22]. The approach presented here can also be applied to other magnetogenesis scenarios with pseudo-scalar seeds such as in string cosmology [23] where coupling to axions may lead to larger helicities.

ACKNOWLEDGMENTS

I would like to thank A. Buonanno, K. Jedamzik, M. Sakellariadou, K. Subramanian, and T. Vachaspati for helpful discussions and comments.

[1] For a review see, e.g., D. Grasso and H. Rubinstein, Phys. Rep. **348**, 163 (2001).
[2] See, e.g., D. Lemoine and M. Lemoine, Phys. Rev. D **52**, 1955 (1995); R. Durrer and M. Sakellariadou, *ibid.* **62**, 123504 (2000).
[3] R. Jackiw and S.-Y. Pi, Phys. Rev. D **61**, 105015 (2000).
[4] J.M. Cornwall, Phys. Rev. D **56**, 6146 (1997)
[5] T. Vachaspati, Phys. Rev. Lett. **87**, 251302 (2001).
[6] See, e.g., K. Enqvist, Int. J. Mod. Phys. D **7**, 331 (1998).
[7] D.T. Son, Phys. Rev. D **59**, 063008 (1999).
[8] G.B. Field and S.M. Carroll, Phys. Rev. D **62**, 103008 (2000).
[9] See, e.g., M. Hindmarsh, M. Christensson, and A. Brandenburg, astro-ph/0201466.
[10] See, e.g., R. Choudhuri, *The Physics of Fluids and Plasmas: An Introduction for Astrophysicists* (Cambridge University Press, Cambridge, England, 1999).
[11] K. Subramanian, Phys. Rev. Lett. **83**, 2957 (1999); **83**, 2957 (1999).
[12] E.W. Kolb and M.S. Turner, *The Early Universe* (Addison-Wesley, Redwood City, CA, 1990).
[13] J. Ahonen and K. Enqvist, Phys. Lett. B **382**, 40 (1996).
[14] K. Jedamzik, V. Katalinic, and A. Olinto, Phys. Rev. D **57**, 3264 (1998).
[15] W.H. Press, S.A. Teukolsky, W.T. Vetterling, and B.P. Flannery, *Numerical Recipes in Fortran* (Cambridge University Press, Cambridge, England, 1992).
[16] G. Sigl, A. Olinto, and K. Jedamzik, Phys. Rev. D **55**, 4582 (1997); M. Joyce and M. Shaposhnikov, Phys. Rev. Lett. **79**, 1193 (1997).
[17] L. Pogosian, T. Vachaspati, and S. Vinitzki, Phys. Rev. D **65**, 083502 (2002).
[18] A. Loeb and A. Kosowsky, Astrophys. J. **469**, 1 (1996).
[19] K. Subramanian and J.D. Barrow, Phys. Rev. Lett. **81**, 3575 (1998).
[20] K. Jedamzik, V. Katalinic, and A. Olinto, Phys. Rev. Lett. **85**, 700 (2000).
[21] C. Caprini and R. Durrer, Phys. Rev. D **65**, 023517 (2002).
[22] For a review see, e.g., P. Bhattacharjee and G. Sigl, Phys. Rep. **327**, 109 (2000).
[23] M. Sakellariadou and G. Sigl (in preparation).